Microstructure Evolution and Fracture Mechanism of 55NiCrMoV7 Hot-Working Die Steel during High Temperature Tensile

Yasha Yuan , Wenyan Wang * , Ruxing Shi , Yudong Zhang , Jingpei Xie

Posted Date: 18 May 2023

doi: 10.20944/preprints202305.1342.v1

Keywords: 55iCrMoV7 steel; hot- working die steel; microstructure evolution; high temperature fracture mechanism; carbides

Article

Microstructure Evolution and Fracture Mechanism of 55NiCrMoV7 Hot-Working Die Steel During High Temperature Tensile

Ya-Sha Yuan [1,2], Wen-Yan Wang [1,*], Ru-Xing Shi [2], Yu-Dong Zhang [2], Jing-Pei Xie [1]

[1] School of Materials Science and Engineering, Henan University of Science and Technology, Luoyang 471023, China;
[2] Luo Yang CITIC HIC Casting and Forging Co Ltd, Luo Yang 471039, China;
* Correspondence: wen210712@163.com

Abstract: In this paper, through high-temperature tensile tests of 55NiCrMoV7 steel, the high-temperature fracture behavior, microstructure evolution and carbide distribution characteristics of both thermal-mechanical coupling zone (fracture zone) and thermal stress zone (clamping zone) at different temperatures were studied. Intrinsic relationship between high temperature fracture and carbides types, distribution and size were revealed and evolution mechanism of microstructure near cracks in 55NiCrMoV7 hot-working die steel during high temperature deformation was clarified. Samples were stretched at different temperatures from 25 °C to 700 °C, and microscopic examinations were carried out by using SEM and TEM. The results showed that: With the increase of temperature, tensile strength and yield strength decreased, elongation and reduction of area increased, and fracture mode changed from brittle fracture to ductile fracture by transition temperature at about 400℃. During high temperature deformation, the grain dislocation density decreased, the tempered martensite decomposed, recovered, recrystallized, and then grain grew. M7C3 and M23C6 carbides precipitated and grew along the grain boundary, and a small amount of fine granular MC carbides were dispersed in the grain. The work done by the external force on the deformation zone would cause the temperature of it to be higher than tensile temperature, which provides thermodynamic conditions for the re-dissolution of small carbides near the fracture zone and the grain growth of large carbides, resulting in the decrease of small carbides and increase of large carbides in thermal-mechanical coupling zone.

Keywords: 55iCrMoV7 steel; hot- working die steel; microstructure evolution; high temperature fracture mechanism; carbides

1. Introduction

Hot-working die steel is used to form high-temperature solid or liquid metal [1,2]. Since die cavity is in direct contact with the high-temperature metal, and also huge mechanical stress, strong friction caused by the flow deformation of hot metal, thermal stress caused by the alternating action between hot metal and cooling medium, hot-working die steel is easy to fail during high temperature service [3–5]. 55NiCrMoV7 is a kind of hot-working die steel with high strength and wear resistance, good impact resistance and tempering stability, and is widely used in die for forgings such as aviation, military, and automobile [6,7]. As the die industry develops in the direction of large-scale, complex, precise, high-efficiency, and fast-paced, its service environment is becoming more and more harsh, which puts forward higher requirements for die materials [8,9]. Many scholars had improved the mechanical properties of die steel by microalloying, adjusting heat treatment process, laser cladding, etc., and had achieved good results. Zhang et al. [10] found that adjusting the content of Mo and V in 5CrNiMo and adding a small amount of Nb could increase the MC content in the steel, thereby greatly improving the high temperature thermal stability of the material. Babu et al. [11] adopted cryogenic heat treatment method [12] to significantly improve the thermal stability and

 doi:10.20944/preprints202305.1342.v1

fatigue properties of steel. Telasang et al. [13–15] believed that laser cladding could greatly improve the hardness, friction and wear properties of die steel.

As we all know, mechanical properties are not only related to the original microstructure before stretching, but also closely related to the microstructure at fracture, second phase type, size, etc. At present, there are many researches on the high-temperature mechanical properties analysis of the tempered microstructure of materials, but less on the microstructure evolution during high-temperature deformation [16]. In this paper, the mechanical properties of 55NiCrMoV7 steel at different tensile temperatures were studied, and the microstructure near the fracture and in the thermal stress zone were systematically analyzed, so as to better understand their microstructure evolution during high temperature service and fracture mechanism during high temperature deformation. The results have theoretical guiding significance for the development of high-strength, large-scale, high-end hot-working die steel under harsh service environments.

2. Experimental Materials and Procedure

2.1. Materials and Heat Treatment

The type of steel material used in the test was 55NiCrMoV7 with chemical components shown in Table 1. The material preparation process was as follows: Smelting 50 Kg steel ingot in vacuum induction furnace-Annealing-Cutting water riser-Forging-Stress relief annealing.

The microstructure of 55NiCrMoV7 steel after heat treatment according to the process of Figure 1 was composed of tempered martensite with high-density dislocations, a small amount of recrystallized ferrite sub-grain and three kinds of carbides, which sizes and types are: 30nm MC, 40~60nm M_7C_3 and $M_{23}C_6$.

Table 1. Chemical compositions of the tested 55NiCrMoV7 steel（weight percent）.

C	Si	Mn	S	P	Cr	Ni	Mo	V
0.56	0.20	0.81	0.0010	0.0065	1.15	1.78	0.52	0.10

2.2. Mechanical Properties

Tempered tensile samples which dimensions and demonstration shown in Figure 2 were prepared under room temperature and high temperature according to GB/T4338. Room temperature and high temperature tensile tests were carried out with DDL300 high-temperature electronic universal testing machine under tensile temperatures of 25 °C, 100 °C, 200 °C, 300 °C, 400 °C, 500 °C, 600 °C and 700 °C. Tensile test used a high temperature resistance furnace with temperature difference of ±3°C to heat the sample. After reaching set temperature, samples were kept for 20 minutes to ensure that the temperature of the surface and the core are uniform. After this heat preservation, tensile tests were carried out at speed of 1mm/min, and samples were air cooled after broken. Three samples were tested at each temperature and the average value was taken. After the test, the tensile strength, yield strength were obtained. Elongation and reduction of area were calculated from the difference between effective gauge length and diameter of the tensile samples before and after the test. A-area of the sample was thermal stress zone and B-area was thermal-mechanical coupling zone as shown in Figure 2.

2.3. Characterization of Microstructure

In order to observe the structural changes near fracture, a small metallographic sample near the fracture perpendicular to the tensile direction (B-area in Figure 2) was taken out and prepared after mechanical grinding, polishing, and 4 % nitric acid alcohol corrosion. The tensile fracture morphology and microstructure of the samples were observed by SM-5610LV SEM. JEM-2100 HRTEM TEM was used to analyze the microstructure of different type, size and distribution of second phase. Carbide size was characterized by Imgae Pro Plus.

Preprints (www.preprints.org) | NOT PEER-REVIEWED | Posted: 18 May 2023 doi:10.20944/preprints202305.1342.v1

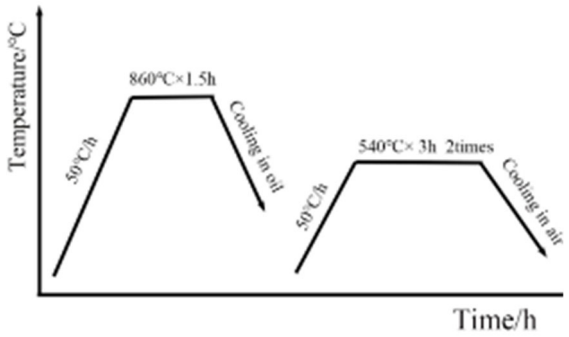

Figure 1. Temperature-time curve of quenching and tempering process.

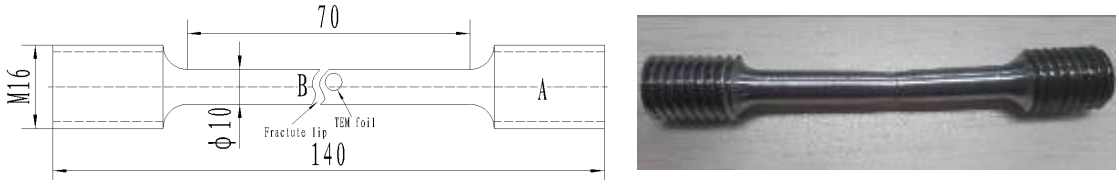

Figure 2. Dimensions and demonstration of tensile samples.

3. Result and Discussion

3.1. High Temperature Mechanical Properties of 55NiCrMoV7 Steel

Figure 3 showed the high temperature performance curves of 55NiCrMoV7 steel at different tensile temperatures after oil cooling for 860 ℃×1.5h and secondary tempering for 540 ℃×3h. It could be seen from the figure that the tensile strength of 55NiCrMoV7 steel was the highest at room temperature, which was 1490Mpa. With the increase of temperature, the tensile strength decreased. It decreased slightly when the temperature was lower than 400 °C while the it decreased rapidly when the temperature exceeded 400°C. The tensile strength was only 107Mpa at 700℃. The trend of high temperature tensile yield strength of 55NiCrMoV7 steel was similar to that of tensile strength. The difference between tensile strength and yield strength was only 17Mpa at 700℃. On the contrary, the elongation and reduction of area increased with the increase of temperature. When temperature exceeded 400 ℃, the increasing rate increased significantly, and the elongation and reduction of area increased from 11 % and 25 % at room temperature to 47 % and 90 % at 700°C respectively.

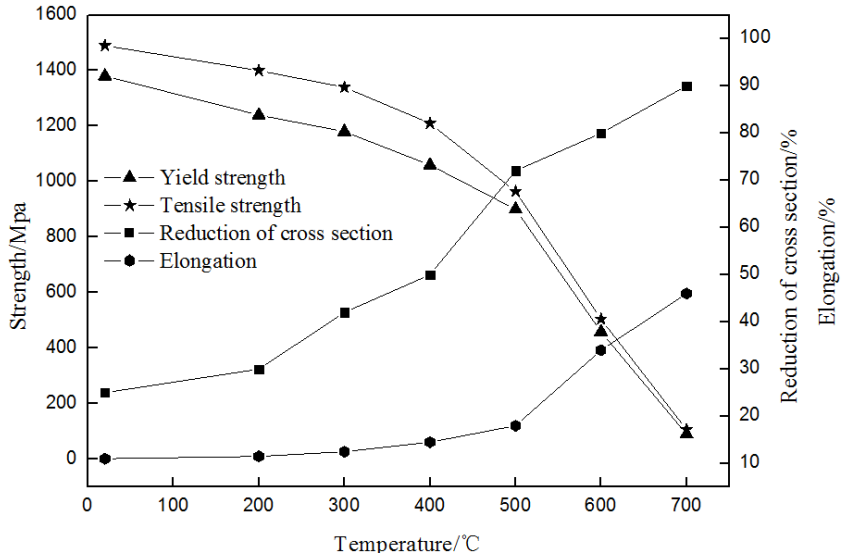

Figure 3. Curve of high temperature mechanical properties of 55NiCrMoV7 steel.

Preprints (www.preprints.org) | NOT PEER-REVIEWED | Posted: 18 May 2023 doi:10.20944/preprints202305.1342.v1

3.2. High Temperature Tensile Fracture Morphology

Figure 4 showed the fracture morphologies of 55NiCrMoV7 steel at different tensile temperatures. It could be seen from Figure 4a that the tensile fracture at room temperature had no obvious necking phenomenon, and the fracture was relatively flat and perpendicular to the tensile axis. There were secondary cracks in the fracture, which started at the center of the sample. Under tensile stress, the cracks rapidly expanded from the center of the sample and broke instantaneously. The fracture was mainly composed of a large number of cleavage planes and a few shear-like dimples [17]. The room temperature tensile fracture of 55NiCrMoV7 steel was brittle fracture.

The high temperature tensile fracture of 55NiCrMoV7 steel exhibited obvious ductile fracture characteristics such as necking and cup-cone. When the tensile temperature was 400 ℃, the crack initiation zone, crack propagation zone and the shear lip zone could be clearly observed, among which the crack propagation zone occupied the largest fracture area, and a large number of equiaxed dimples with size of 0.8~1.2μm could be seen in the fracture. When the stretching temperature increased from 400℃ to 500℃, a few 1.8-2.6μm plastic pores appeared in the fracture, while the rest of the fracture characteristics did not change much. The fracture area was reduced, which was consistent with the higher reduction of area at 500 °C in Figure 3. When the tensile temperature rise to 600 °C, tensile deformation caused the cross-section to be at 45° angle to the tensile direction, resulting in shear stress. With the increase of stress, crack propagation, penetration and failure occurred, and the plastic deformation characteristics near fracture were more obvious, at the same time, a large number of scaly slippage bands appear on the surface of the specimen near the fracture. Compared with low temperature, the dimple depth in the fracture became deeper, dimple size increased obviously and showed obvious ductile fracture which was consistent with the low strength, high toughness results shown in Figure 3 at this temperature.

From fracture analysis at different tensile temperatures, it could be concluded that as the tensile temperature increased, the tensile fracture changed from brittle fracture to ductile fracture, dimple numbers gradually decreased, dimple sizes became larger from 0.8–1.2μm at 400 °C to 2.8–4.2μm at 600 °C.

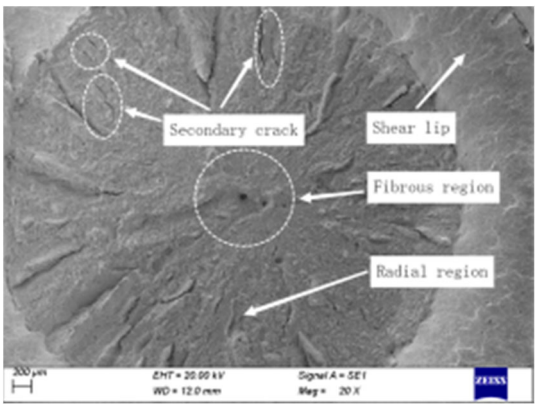

(**a**)

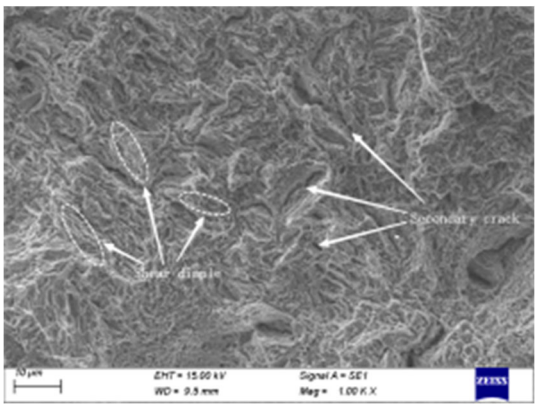

(**b**)

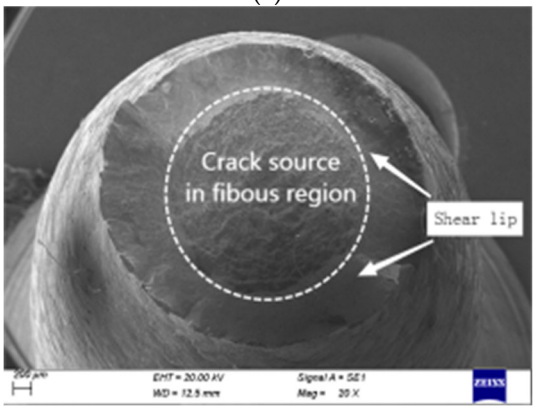

(**c**)

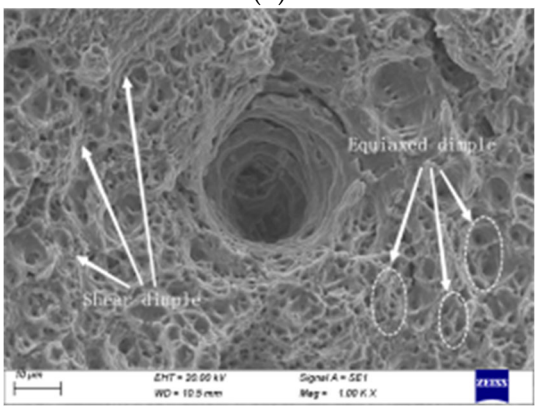

(**d**)

Preprints (www.preprints.org) | NOT PEER-REVIEWED | Posted: 18 May 2023 doi:10.20944/preprints202305.1342.v1

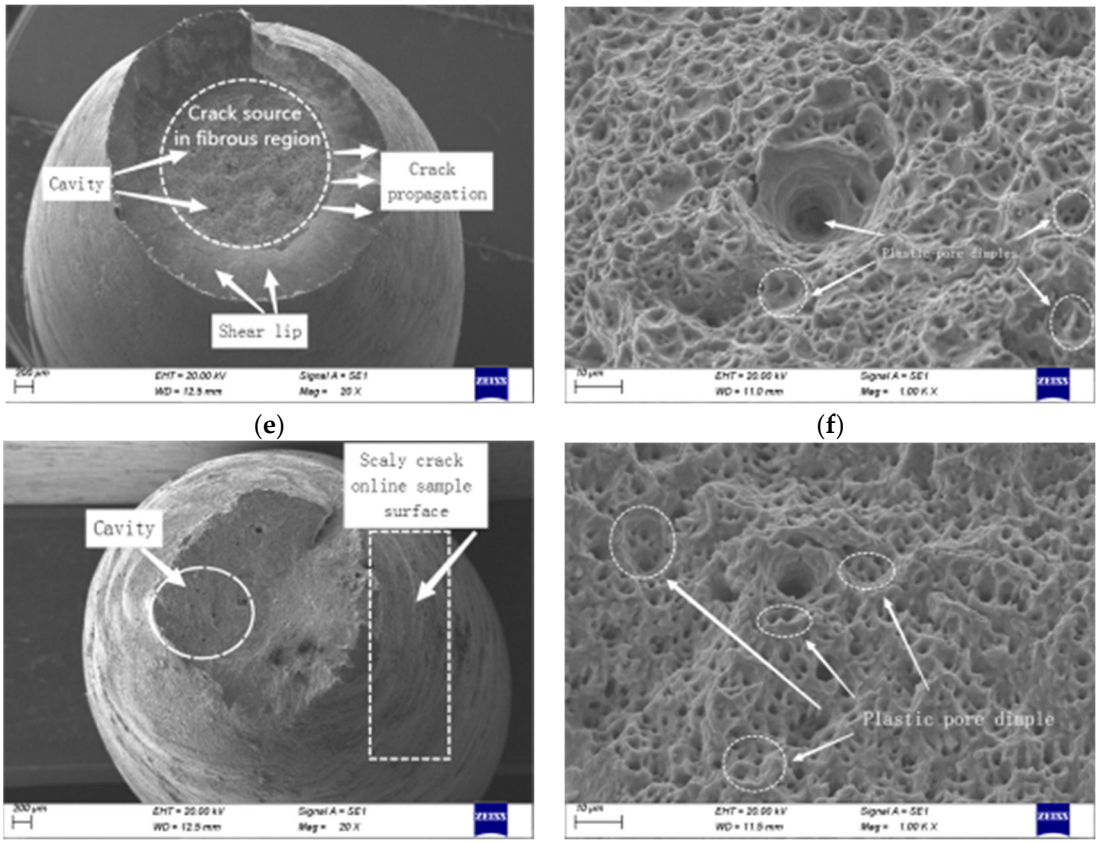

Figure 4. Tensile fracture morphology of 55NiCrMoV7 steel at different temperature. (a)(b)Room temperature; (c)(d)400 ℃; (e)(f)500 ℃; (g)(h)600 ℃.

Table 2 showed the statistical results of the area of fracture crack propagation zone and crack initiation zone at different tensile temperatures. It could be seen that the area of the crack propagation zone in the fracture at different temperatures was larger than the area of the crack initiation zone, and there was a positive correlation between the two areas and the tensile strength of steel. Larger two areas could effectively hinder the formation and propagation of cracks and improve crack formation energy. Under tensile stress, the crack reached the instantaneous breaking area, and rapidly expanded and broke along the direction of the maximum shear force. Therefore, large area of the crack initiation area and crack propagation area was beneficial to improve high temperature tensile strength of steel, which was consistent with the mechanical properties at high temperature shown in Figure 3.

Table 2. Statistical results of the area of fracture crack propagation zone and crack initiation zone.

Tensile temperature /℃	The area of fracture crack propagation zone/mm²	The area of crack initiation zone/mm²	The total area/mm²
Room temperature	16.05	2.10	18.15
400℃	6.94	0.92	7.86
500℃	5.43	0.69	6.12
600℃	3.08	0.31	3.39

Preprints (www.preprints.org) | NOT PEER-REVIEWED | Posted: 18 May 2023 doi:10.20944/preprints202305.1342.v1

3.3. Effect of Tensile Temperature on Microstructure of 55NiCrMoV7 Steel

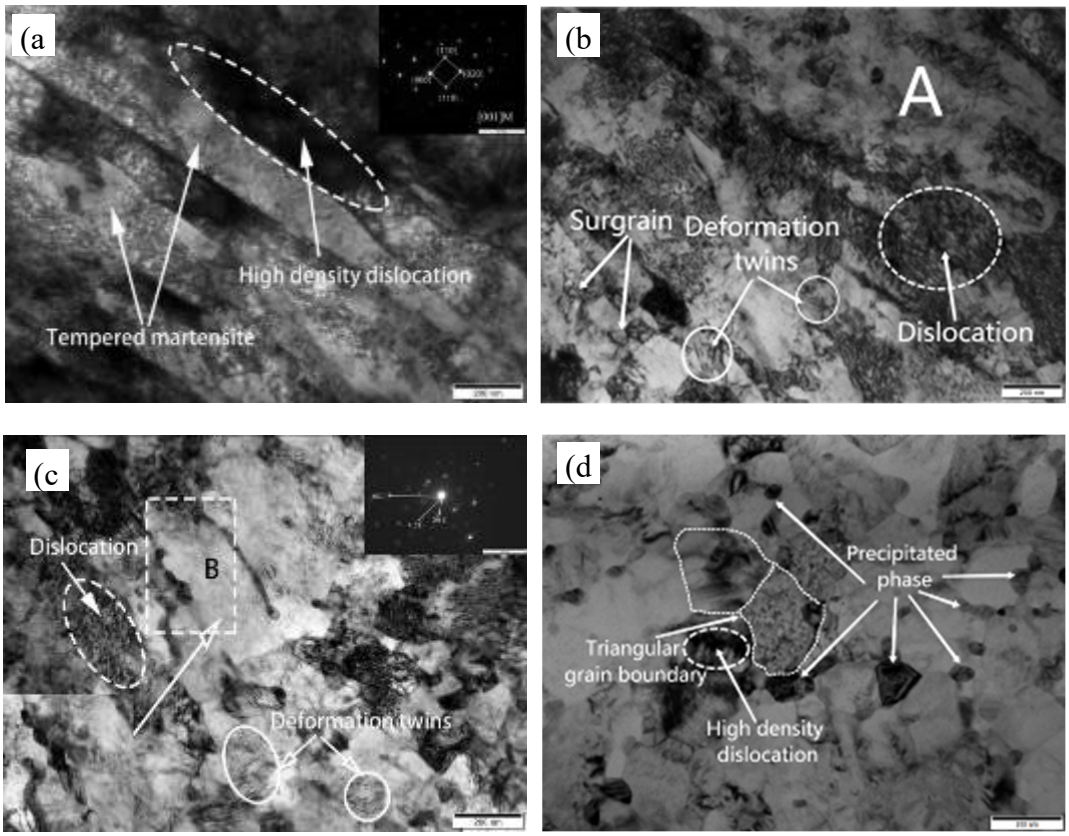

Figure 5. TEM images of 55NiCrMoV steel near the fracture at different tensile temperatures. (a)Room temperature; (b)400 °C; (c)500 °C; (d)600 °C.

Figure 5 showed the TEM images of 55NiCrMoV7 steel near the fracture at different tensile temperatures. It could be seen from the figure that the microstructure was tempered lath martensite with a width of about 160 nm and a length of 1600 nm after stretching at room temperature. There were a large number of high-density dislocations distributed in the martensite, and dislocation slip could only happen in a limited distance, which was the main reason for the high strength and low toughness of 55NiCrMoV7 steel at room temperature.

At stretching temperature of 400 °C, the tempered lath martensitic still existed in some areas (shown in Area A in Figure 5b). A small amount of deformed twin-crystals could be observed in the tempered martensite beam, which had a significant effect on improving the plasticity and toughness of the material. Compared with room temperature stretching, the dislocation density and the degree of dislocation entanglement were significantly reduced, and 20-50 nm subgrains formed by recovery and recrystallization were found in some regions.

When stretching temperature was further increased to 500℃, dislocation density was also further reduced, supersaturated carbon was redistributed in the tempered lath martensite, and the recovery-recrystallization phenomenon was more obvious, all resulting in a significant decrease in the strength of the material. A large number of twin-crystals appeared in the grains and showed obvious recrystallization phenomenon. According to the diffraction spot(shown in the upper right corner of Figure 5c), it could be seen that a large number of α-phase polycrystalline diffraction rings were formed at this temperature, and dislocation density was significantly reduced. Only a small part of the remaining martensite showed wave-like discontinuous tempering deformation characteristics, which were strong evidences of strength reduction under high temperature tensile. A large number of equiaxed-grains in the microstructure were produced by grain breakage and recrystallization under high temperature tensile stress, and the second phase was preferentially precipitated at the martensite lath boundary (shown in lower left corner of Figure 5c and Area B), reducing the

 doi:10.20944/preprints202305.1342.v1

continuity between grains. Under tensile stress, the stress concentration around the second phase weakened the grain boundary strengthening effect, accelerated the crack propagation, and reduced the strength of the material.

When the stretching temperature reached 600°C, the recovery and recrystallization of tempered martensite were basically completed, the sub-grains formed by recrystallization grew significantly, dislocations basically disappeared, only a small amount of high-density dislocations existed at local trigeminal grain boundaries. The number and size of carbides precipitated along the grain boundary increased significantly.

3.4. Precipitate Phase Analysis

Figure 6 showed TEM images and selected electron diffraction pattern of $M_{23}C_6$, M_7C_3 and MC carbides in 55NiCrMoV7 steel when stretched at 500 °C. It could be seen from the figure that carbides with 30-70nm width and 100nm length elongated along the grain boundaries were precipitated at the grain boundaries. It could also be seen from Figure 6c that there were sharp-angle precipitates with a width of about 100nm and length of 200nm at the intersection of the martensitic lath boundary. Through the calibration of the electron diffraction pattern, they were $M_{23}C_6$ carbide and M_7C_3 carbide mainly containing Cr respectively (Figure 6a,b,d). Compared with M_7C_3 (40~60 nm) in unstretched 55NiCrMoV7 steel, the carbides grew significantly under tensile stress at high temperature. This was mainly due to the fact that under the tensile stretch at 500°C, the tempered martensite underwent the decomposition-recovery-recrystallization process, and the dislocations were pushed to the surrounding grain boundaries to form dislocation walls, which provided dynamic conditions for precipitation and growth of carbides at grain boundaries. The work done by the external force on the deformation zone during high temperature stretching would cause the temperature of it to be higher than tensile temperature, which provided thermodynamic conditions for the re-dissolution of small carbides near the fracture zone and the grain growth of large carbides. Due to the low thermal activation energies of M_7C_3 and $M_{23}C_6$ carbides [18,19], Cr-containing carbides had grew significantly during high temperature stretching.

It could be seen from Figure 6e that there were small and dispersed carbides in the grains, with a size of about 30nm. It could be seen from the electron diffraction pattern that they were MC carbides (Figure 6f). They were similar to the size of MC in unstretched 55NiCrMoV7 steel, which was mainly due to the larger growth activation energy and higher thermal stability of MC carbides [20].

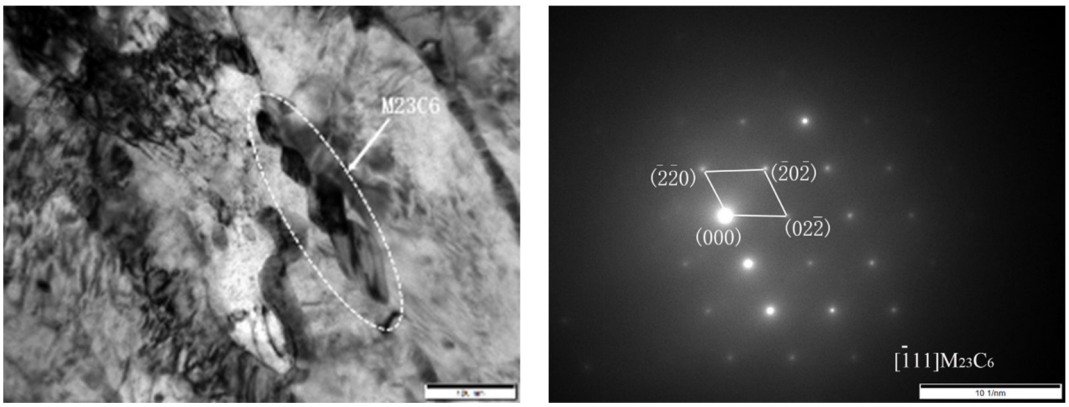

(**a**) (**b**)

Preprints (www.preprints.org) | NOT PEER-REVIEWED | Posted: 18 May 2023 doi:10.20944/preprints202305.1342.v1

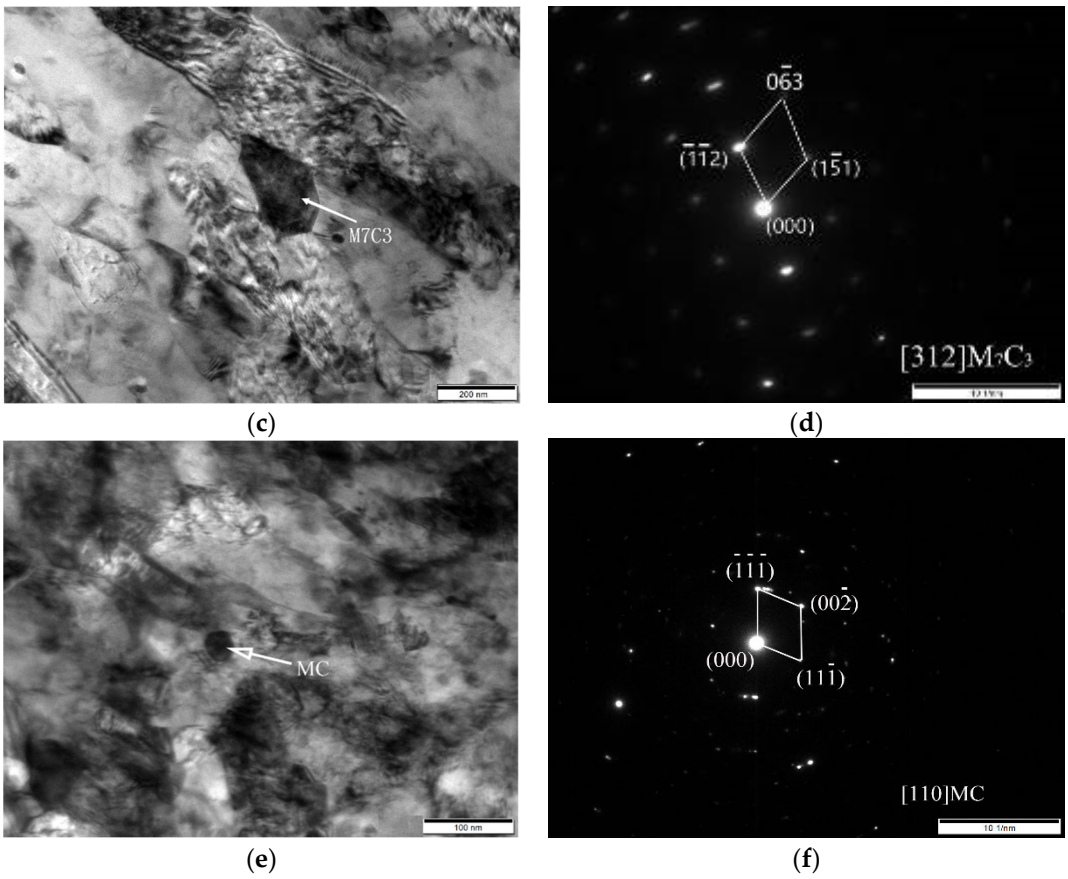

Figure 6. TEM images and selected electron diffraction pattern of precipitated phase of 55NiCrMoV steel at 500 °C stretching (a) Bright-field image of $M_{23}C_6$; (b) selected electron diffraction pattern of $M_{23}C_6$; (c) Bright-field image of M_7C_3; (d) selected electron diffraction pattern of M_7C_3; (e) Bright-field image of MC; (f) selected electron diffraction pattern of MC.

3.5. Microstructure of Thermal Stress Zone and Thermal-Mechanical Coupling Zone of High Temperature Stretching Samples

Figure 7 showed microstructure of thermal stress zone and thermal-mechanical coupling zone at different stretching temperatures. When tensile temperature was 400℃, the microstructure of the thermal stress zone was composed of tempered martensite and a small amount of nano-sized carbides. Under tensile stress, the microstructure of the thermal-mechanical coupling zone showed obvious deformation and directionality. When tensile temperature reached 600℃, the large carbides increased significantly and grew. Martensite decomposed, the microstructure appeared obvious recrystallization, and the ferrite content increased slightly. Compared with the thermal stress zone, plastic deformation in the thermal coupling zone was more obvious, small carbides are reduced, large carbides increased, and the morphology was relatively round. The fine granular carbides had high chemical potentials, which were prone to Ostwald ripening under high temperature tensile stress, and were easily redissolved in the matrix or diffused into the large carbides to cause reduction of carbon and alloying elements in grains. With the transformation of highly coherent carbides to low coherent or incoherent carbides [21–23], the 55NiCrMoV7 steel matrix exhibited obvious softening, which was also the reason for the decrease in strength and the increase in plasticity under the tensile temperature of 600 °C.

Preprints (www.preprints.org) | NOT PEER-REVIEWED | Posted: 18 May 2023 doi:10.20944/preprints202305.1342.v1

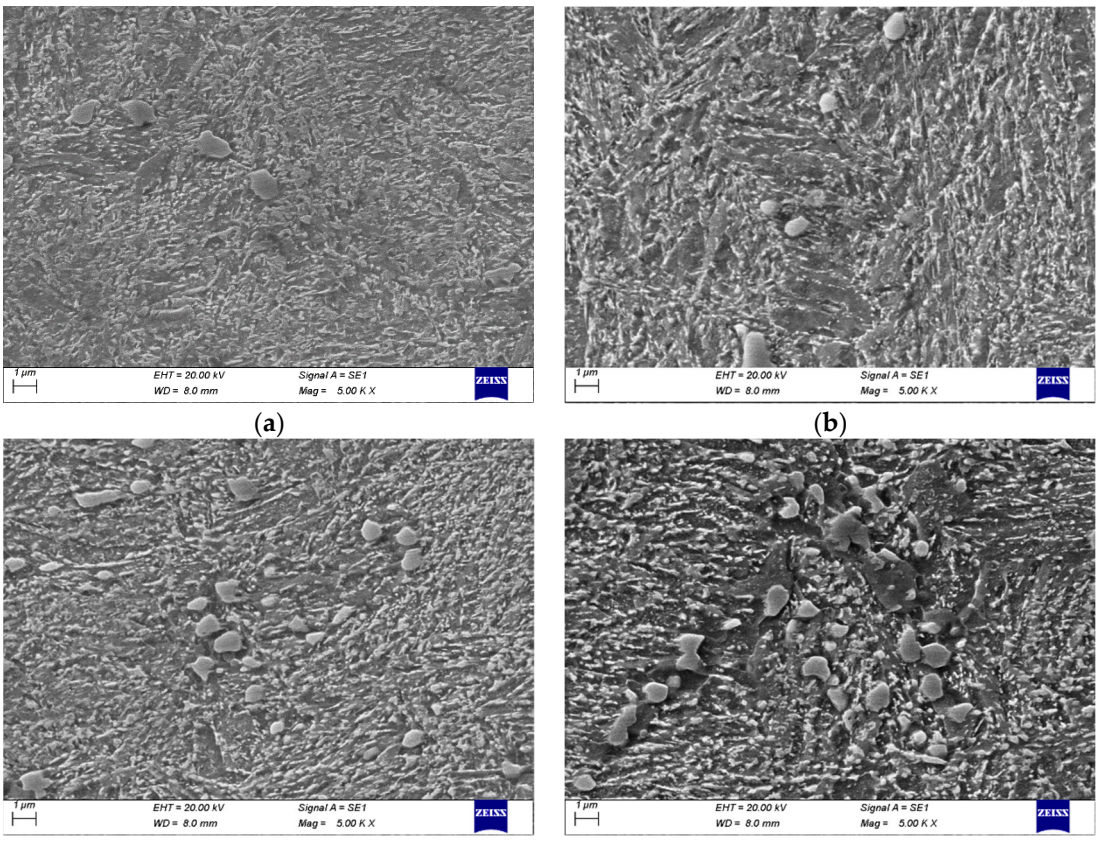

Figure 7. Microstructure of thermal stress zone and thermal-mechanical coupling zone at different stretching temperatures (a) Thermal stress zone at 400 ℃; (b) Thermal-mechanical coupling zone at 400 ℃ (c) Thermal stress zone at 600 ℃; (d) Thermal-mechanical coupling zone at 600 ℃.

Figure 8 showed the number and size of carbides in the thermal stress zone and thermal-mechanical coupling zone under different conditions. It could be seen from the figure that the number of small carbides in the thermal-mechanical coupling zone was less than that in thermal stress zone, thermal-mechanical coupling effect leaded to a reduction of carbides. Compared with different temperatures, there were more small carbides and less large carbides in thermal stress zone and the thermal-mechanical coupling zone at 400℃ than that of 600℃. Comparing the thermal stress and thermal-mechanical coupling zone, it could be seen that small carbides below 0.2×10²nm were redissolved under thermal-mechanical coupling, the number of (0.2~1.0)×10²nm carbides was significantly reduced, the number of (1.0~1.5) ×10²nm carbides remain unchanged. The sharp corners of large carbides decomposed and gradually became rounded, and the percentage of carbides above 2.0×10²nm increased significantly.

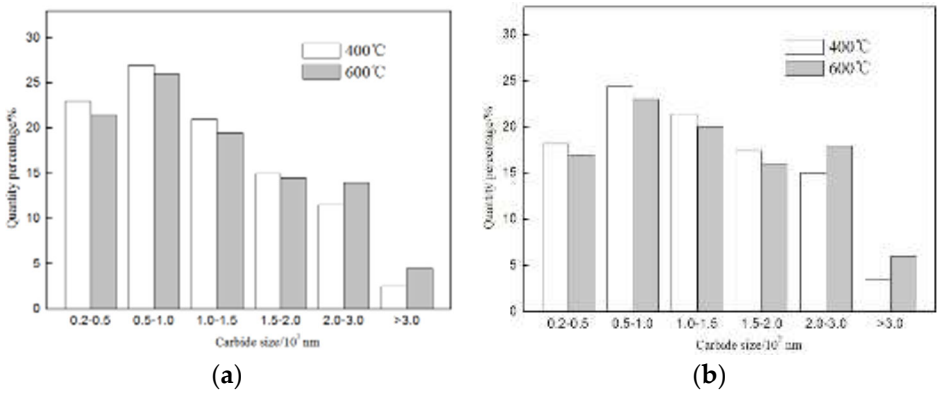

Figure 8. Carbide size distribution of 55NiCrMoV7 steel at different tensile temperatures (a) Thermal stress zone; (b) Thermal-mechanical coupling zone.

 doi:10.20944/preprints202305.1342.v1

Under thermal-mechanical coupling effect, the dislocation proliferation caused by tensile deformation provided a channel for the diffusion of carbon atoms and alloying elements. At 600℃, the strengthening effect of solid solution and dislocation weakened, which leaded to the increase of plasticity of steel, the tensile deformation and the tensile force formed an angle of 45°resulting in shear stress. Small carbides redissolved, large carbides aggregated to form clusters, and the matrix between clusters had no carbide pinning dislocations. Due to the soft matrix, large and deep plastic pores were formed under tensile stress. Therefore, the steel had high elongation and reduction of area at 600℃.

When the temperature increased from 400℃ to 600℃, the solid solution strengthening and dislocation strengthening of the steel weakened, resulting in a decrease in strength and increase in plasticity of the steel. The bonding energy between metal atoms decrease the discontinuous stress distribution between carbide and matrix leaded to uneven deformation of the steel, and the fracture morphology showed dimples with different depths. With the increase of tensile temperature, the dislocation density decreased obviously, the precipitated carbides grew up, and under tensile stress, cracks began to initiate near the carbides. Without the strengthening effect of high-density dislocations, the carbides were insufficient to withstand large stresses and break, which was consistent with the results of low-strength, high-plastic at 600 °C (Figure 3).

3.6. Effect of Carbides on Crack Initiation and Propagation

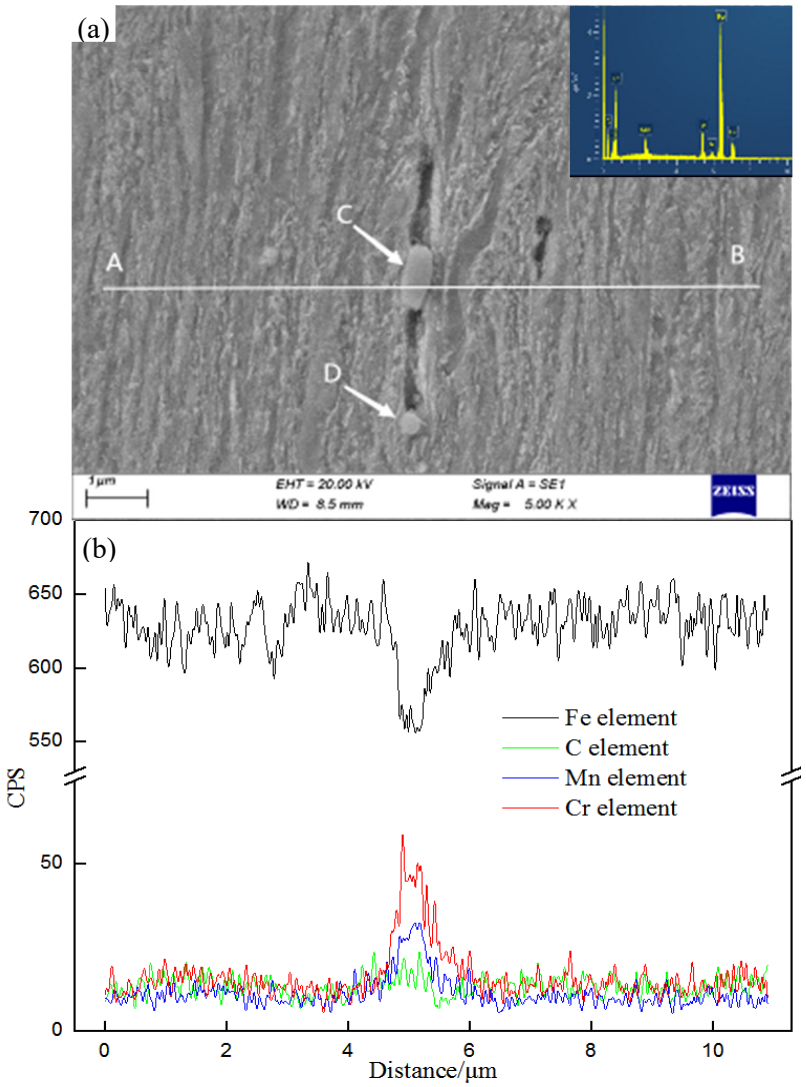

Figure 9. Line scanning of Fe, C, Mn and Cr elements near the crack in 55NiCrMoV7 steel. (a) SEM image of crack propagation; (b) Line scaning and elements EDS results

 doi:10.20944/preprints202305.1342.v1

In order to further obtain the relationship between carbides and crack initiation and propagation, the microstructure and potential cracks of the 500°C tensile samples near the fracture were studied in detail. As shown in Figure 9: There were cracks of different lengths near the fracture and one of the long cracks was analyzed. There were approximately rod-shaped (irregular shape and small sharp corners) and spherical carbides distributed in the middle and end of the crack respectively. The composition changes and distributions of Fe, C, Cr, and Mn shown in Figure 9b were obtained by performing line scanning through the rod carbide along AB line in Figure 9a. The composition change and distribution of Fe, C, Mo and V shown in the upper right corner of Figure 9a were obtained by EDS energy spectrum analysis of the D carbide in Figure 9a. According to the distribution of alloying elements and previous tests, the rod-shaped carbide C was $M_{23}C_6$ or M_7C_3 carbide mainly containing Cr and Mn, and the spherical carbide D was MC carbide mainly containing Mo and V. It could be seen from the figure that when the crack started near the $M_{23}C_6$ carbide, the crack continued to expand along the C carbide interface, and when the crack extended near D carbide, the crack stopped to expand, indicating that the approximate spherical MC carbide had a blocking effect on the crack propagation.

In Cr-Mo-V materials, $M_{23}C_6$ and M_7C_3 carbides maintain noncoherent relationship with the matrix with low thermal activation energy. Under mechanical and thermal stress, they precipitated along the grain boundary and were easy to grow up. Due to irregular shape, stress concentration was easy to occur at sharp corners and crack sources generated easily. MC carbides were finely dispersed in the matrix, and their shape was nearly spherical, which was not conducive to stress concentration. MC carbides maintained a coherent relationship with the matrix, had high thermal activation energy, were not easy to grow, could pin dislocations, hindered dislocation movement, reduced stress concentration generated by dislocations at large particle carbides, and effectively prevented crack initiation and propagation.

4. Conclusion

(1) With tensile temperature increased from room temperature to 700°C, the tensile strength of 55NiCrMoV7 steel decreased from 1490Mpa to 107Mpa, and the elongation and reduction of area increased from 11 % and 25 % to 47 % and 90 % respectively. When stretching temperature was higher than 400°C, the decrease rate of strength and the increase rate of plasticity increased significantly.

(2) In this experiment, the tensile fracture of 55NiCrMoV7 steel changed from brittle fracture to ductile fracture by transition temperature of 400°C. The dimple size gradually increased from 0.8-1.2μm at 400°C to 2.8-4.2μm at 600°C with the increase of tensile temperature.

(3) The microstructure under room temperature stretching was mainly lath martensite with large amount of high-density dislocations distributed inside. During high temperature deformation process, the microstructure showed obvious recovery and recrystallization, and the dislocation density decreased. The M_7C_3 and $M_{23}C_6$ carbides that are incoherent to the matrix precipitated and grew along the grain boundaries, while other MC carbides that are coherent to the matrix were dispersed in the grains.

(4) Under high temperature tensile stress, stress concentration was easily generated around the M_7C_3 and $M_{23}C_6$ carbides precipitated along the grain boundary, which weakened the strengthening effect of the grain boundary and accelerated the crack propagation, while the granular MC carbides dispersed in the grain could prevent cracks. Therefore, reducing M_7C_3 and $M_{23}C_6$ carbides content and increasing other MC carbides content were beneficial to improve high temperature performance of hot-working die steel.

(5) During high temperature stretching, the work done by the external force on the deformation zone would cause the temperature of it to be higher than tensile temperature, which provides thermodynamic conditions for the re-dissolution of small carbides near the fracture zone and the grain growth of large carbides, resulting in the decrease of small carbides and increase of large carbides in thermal-mechanical coupling zone.

Acknowledgement The authors acknowledge with gratitude funding received from National Key R&D Program of China (Grant No.2020YFB2008400).

Conflict of Interest: The authors (Ya-Sha Yuan, Wen-Yan Wang, Ru-Xing Shi, Yu-Dong Zhang, Jing-Pei Xie) declare that we have no financial and personal relationships with other people or organizations that can inappropriately influence our work, there is no professional or other personal interest of any nature or kind in any product, service and/or company that could be construed as influencing the position presented in, or the review of, the manuscript entitled, "Microstructure evolution and fracture mechanism of 55NiCrMoV7 hot-working die steel during high temperature tensile"

References

1. WU XC, SHI YJ (2015) Development status and trend of hot forging die materials. Die and Mould Industry 41(8): 1-10.
2. WANG B (2017) Development status of hot work die steel. Die & Mould manufacture 17(02): 79-82.
3. Chen RC, Wang ZQ, Wang HB，Liang Q, Zhu FS (2021) Effects of yttrium on the microstructures, internal fraction and martensitic transformation in H13 die steel. Journal of Materials Science 56: 7753-7764.
4. WU XC, ZUO PP (2013) Development status and trend of hot working die steels at home and abroad. Die & Mould industry 39(10): 1-9.
5. Zhang YQ, Zhang C, Li F et al (2022) High-Temperature Oxidation Behavior of Cr-Ni-Mo Hot-Work Die Steels. Materials (Basel, Switzerland) 15(15):5145-5145.
6. WANG SQ, ZHU T, MAO YS (2012) Wear resistance and wear mechanism of hot-forging die steels. Materials Science & Technology 20(02): 140-144.
7. Zhu J, Zhang ZH, Xie JX (2019) Improving strength and ductility of H13 die steel by pre-tempering treatment and its mechanism. Mater Sci Eng A 752(3): 101-114.
8. Yu XS, Wu C, Shi RX, Yuan YS (2021) Microstructural evolution and mechanical properties of 55NiCrMoV7 hot-work die steel during quenching and tempering treatments. Adv. Manuf. 9: 520-537.
9. Han RQ, Wu XC (2018) Research status and development trend of die steel for plastic material forming at domestic and foreign. Die and Mould Industry 44(9): 1-7 .
10. Hu ZQ, Wang KK (2020) Evolution of Dynamic Recrystallization in 5CrNiMoV Steel during Hot Forming. Advances in Materials Science and Engineering 2020(12): 1-13.
11. Wang SY, Hou XY, Cheng Y, Sun Y, Yang YH, Li JG, Zhang HW, Zhou YZ (2022) Effect of temperature on the tensile deformation behavior and fracture mechanism of a transient liquid-phase bonding joint of γ′-strengthened Co-based single-crystal superalloy. Journal of Materials Science 57(25): 12012-12033.
12. Yan ZJ, Liu K, Eckert J (2020) Effect of tempering and deep cryogenic treatment on microstructure and mechanical properties of Cr-Mo-V-Ni steel. Mater Sci Eng A 787: 1-8.
13. Telasang G, Majumdar JD, Padmanabham G, Manna I (2014) Effect of laser parameters on microstructure and hardness of laser clad and tempered AISI H13 tool steel. Surface & Coatings Technology 258: 1108-1118.
14. Telasang G, Majumdar JD, Padmanabham G, Manna I (2014) Structure–property correlation in laser surface treated AISI H13 tool steel for improved mechanical properties. Materials Science & Engineering A 599:255-267.
15. Telasang G, Majumdar JD, Padmanabham G, Manna I (2015) Wear and corrosion behavior of laser surface engineered AISI H13 hot working tool steel. Surface & Coatings Technology 261: 69-78.
16. Salcedo D, Luis CJ, Luri R, Fuertes JP (2015) Design and Optimization of the Dies for the Isothermal Forging of a Cam. Procedia Engineering 132: 1069-1076.
17. Wen LJ, Hu XG, Li Z, Zhan HW, Wu JK, Zhu Q (2022) Anisotropy in tensile properties and fracture behaviour of 316L stainless steel parts manufactured by fused deposition modelling and sintering. Advances in Manufacturing 3: 1-11.
18. Hu X, Li L, Wu X et al (2006) Coarsening behavior of M23C6 carbides after ageing or thermal fatigue in AISI H13 steel with niobium. Int. J. Fatigue 28(3): 175-182.
19. Tkachev ES, Belyakov AN, Kaibyshev RO (2020) The Role of Deformation in Coarsening of M23C6 Carbide Particles in 9% Cr Steel. Physics of Metals and Metallography 121(8): 804-810.
20. Haglöf F, Kaplan B, Norgren S, Blomqvist A, Selleby M (2019) Experimental study of carbides in the Ti–Cr–C system. Journal of Materials Science 54(19): 12358-12370.

 doi:10.20944/preprints202305.1342.v1

21. Jiang YF, Zhang B, Zhou Y, Ke W (2018) Atom probe tomographic observation of hydrogen trapping at carbides/ferrite interfaces for a high strength steel. Journal of Materials Science & Technology 34(8): 1344-1348.
22. Gope N, Chatterjee A, Mukherjee T (1993) Influence of long-term aging and superimposed creep stress on the microstructure of 2.25Cr1Mo. Metallurgical Transactions A 24(2): 315-326.
23. Cao GH, Zhang DT, Luo XC, Zhang WW, Zhang W (2016) Effect of aging treatment on mechanical properties and fracture behavior of friction stir processed Mg–Y–Nd alloy. Journal of Materials Science 51(16): 7571-7584.